

Arsenate removal from aqueous solutions: thermodynamic and kinetic study on iron hydroxide-impregnated corn cob

Eloísa Stéphanie da Silva ¹, Renata de Castro Pires ², Leandro Vinícius Alves Gurgel ³, Versiane Albis Leão ²

¹ Universidade Federal de Ouro Preto, Graduate Program in Environmental Engineering (eloisa.stephanie@hotmail.com). Campus Morro do Cruzeiro, s.n., Bauxita, Ouro Preto, MG, 35400-000, Brazil

² Universidade Federal de Ouro Preto, Hydrometallurgy Laboratory, Department of Metallurgical and Materials Engineering (versiane@ufop.edu.br), re_cpaires@yahoo.com.br. Campus Morro do Cruzeiro, s.n., Bauxita, Ouro Preto, MG, 35400-000, Brazil.

³ Universidade Federal de Ouro Preto, Department of Chemistry, Institute of Exact and Biological Sciences (legurgel@ufop.edu.br), Campus Morro do Cruzeiro, s.n., Bauxita, Ouro Preto, MG, 35400-000, Brazil

Corresponding author: versiane@ufop.edu.br (Versiane Leão)

Abstract: The contamination of water resources with arsenic is a serious environmental problem. This research investigated the use of a strategic agricultural waste for Brazil, i.e., corn cob as a low-cost, biodegradable, and eco-efficient material for As(V) adsorption. Arsenate removal from an aqueous solution with iron hydroxide impregnated corn cob (IHCC) was investigated under different pH values (2-10). FTIR spectra revealed that monodentate complexes were formed during the adsorption of arsenate on IHCC. Furthermore, SEM micrographs revealed a uniform distribution of Fe(III) and also As(V) on the IHCC. IHCC was efficient in the removal of arsenic from acidic solutions, mainly those having pH values between 2 and 3 at temperatures below 50°C. The adsorption kinetics followed the pseudo-second order model with an activation energy of 39.35 ± 6.99 kJ mol⁻¹ implying that chemical reaction was the controlling step of arsenic adsorption by IHCC. In addition, arsenic adsorption on IHCC was (i) an entropically driven, (ii) spontaneous, and (iii) endothermic phenomenon (+23.82 kJ mol⁻¹) and involved electrostatic adsorption and chemisorption ($Q_{\max} = 40$ mg/g, at 25°C). Therefore, a promising sustainable and environmentally friendly solution for the use of IHCC was devised in the current work.

Keywords: biosorbent, toxic metals, Impregnation, agricultural wastes, mine waters

1. Introduction

Arsenic (As) is a metalloid found in small amounts in rocks, soils, water, and air (WHO, 2023). In the earth's crust, arsenic is present in approximately two hundred types of minerals, mainly sulphides, such as arsenopyrite (FeAsS) (Odling et al., 2020). Inorganic arsenic can be found as arsenite (AsO₃³⁻) or arsenate (AsO₄³⁻) in aqueous environments. Arsenic toxicity depends on its speciation, being the trivalent form the most toxic, which predominates in reducing environments such as anaerobic groundwater whereas the pentavalent species is found in oxidizing environments such as surface waters (WHO, 2001).

Humans are exposed to arsenic contamination mostly by food (70%) and water (30%) intake (WHO, 2023). Several are the adverse effects of the metalloid on the human health include renal and respiratory failure, encephalopathy and/or psychosis, cardiomyopathy, and acute skin rash. whereas long-term exposure to the element can cause bladder, lung, and skin cancers (WHO, 2023, Warwick et al., 2021). Concerns about arsenic contamination in humans have increased following the incident in Bangladesh, where thousands of people were contaminated after consuming arsenic-bearing groundwater (Deschamps and Matschullat, 2007, Smith et al., 2000). Therefore, arsenic contamination has been treated as a serious health issue in Bangladesh, India, China, Pakistan, Mexico, USA, Nepal, New Zealand, Taiwan, Vietnam, Argentina, Chile, Cambodia, Japan, and Brazil, among other countries

(Mohan and Pittman, 2007). Before the 1990s, the standard value established for total arsenic in drinking water was $50 \mu\text{g L}^{-1}$, but considering the high toxicity and carcinogenic potential of the element, this limit was reduced to $10 \mu\text{g L}^{-1}$ (WHO, 2023).

Aiming at reducing the arsenic concentration in drinking and wastewaters, an array of technologies is conventionally employed: (i) co-precipitation with metals (iron and aluminium), (ii) adsorption onto iron-based materials (oxides and hydroxides) and activated alumina, (iii) ion exchange, (iv) phytobial remediation, (v) electrocoagulation, and (vi) reverse osmosis (Alka et al., 2021). The species As(V) can also be removed by adsorption on manganese oxide minerals (Deschamps et al., 2003), acid mine drainage sludge (Byambaa et al., 2021), goethite, and gibbsite (Ladeira and Ciminelli, 2004).

Arsenic adsorption on lignocellulosic biomasses is a promising technology because it employs renewable, efficient, and low-cost materials (Sen Gupta and Bhattacharyya, 2011, Maia et al., 2021). Nevertheless, the use of lignocellulosic biomass to remove arsenic from wastewaters is still poorly investigated (Maia et al., 2021). Usually, the adsorption capacities can be improved by chemical modification (Mohan and Chander, 2006, Sud et al., 2008). In this regard, given the great affinity between arsenic and iron, impregnation with Fe-bearing compounds has been tried to different biomasses such as orange and cellulose wastes, wheat bran, coconut mesocarps, rice husks, sugarcane bagasse, and wheat straw (Ghimire et al., 2003, Dupont et al., 2007, Rijith et al., 2012, Pehlivan et al., 2013a, Pehlivan et al., 2013b, Nashine and Tembhurkar, 2016, Tian et al., 2011). In addition, modified biochars produced from agricultural wastes have been applied to increase the capacity to remove As from waters and wastewaters. Some examples comprise Fe-oxide rice husk (Cope et al., 2014), magnetic-pine wood (Wang et al., 2015), hydrogel rice husk (Sanyang et al., 2016), AIOOH-nano-composite cotton wood (Zhang and Gao, 2013), and nZVI-pine wood (Wang et al., 2017). Although, impregnation is not always successful as some of these materials have low to medium adsorption capacities (between 2.47 m g^{-1} and 22.5 m g^{-1}) (Dupont et al., 2007, Pehlivan et al., 2013a, Pehlivan et al., 2013b, Tian et al., 2011), adsorbents with high adsorption capacities, i.e. 68 mg/g (Ghimire et al., 2003) and 104 mg/g (Rijith et al., 2012) were achieved when orange wastes and coconut mesocarps, respectively, were studied.

Particularly in the case of coconut mesocarp, its selection as adsorbent is justified by the high coconut production in countries such as India, which attained 13.3 Mg in 2021 (Brainer, 2021; Rijith et al., 2012). However, this does not align with the Brazilian reality, as the Brazilian production of corn cobs (85.7 million Mg) (CONAB, 2021) is bigger than that of the two cited wastes (16.7 Mg and 2.4 Mg in 2021, respectively) (Brainer, 2021; Vidal, 2021). In this regard, corn cob is widely available as an inexpensive agricultural waste. Corn is the second most important agricultural commodities produced and marketed in Brazil, second only to soybeans (CONAB, 2021), with only the grain being marketed to produce animal feed and various industrialized products (Schneider et al., 2012). It is estimated that for every 100 kg of threshed corn, the corn cob waste represents about 18 kg (Ziglio et al., 2007). This material is composed mostly hemicelluloses, lignin, and cellulose, and in the latter can be chemical modifications that are responsible for increasing the capacity to biosorb metals (Sud et al., 2008). Another advantage of corn cob is its biodegradability, which makes the process more sustainable as compared to the use of synthetic adsorbents. Therefore, corn cobs impregnated with iron hydroxide can produce a promising biosorbent for removing As(V) from aqueous solutions, offering a cost-effective and efficient solution for treating As-contaminated water.

In the face of the need for efficient, viable, and novel technologies aiming at the removal of arsenic, the current study investigated the application of Fe(OH)₃-impregnated corn cob in the removal of As(V) from aqueous solutions. The effect of the solution pH on arsenic adsorption was evaluated in the pH range between 2 and 10. Infrared spectroscopy was used to elucidate the interaction of As(V) with the adsorption sites. Furthermore, kinetic studies were conducted to determine the rate constant and activation energy associated to the adsorption process. Equilibrium studies and the determination of the thermodynamic parameters of As(V) adsorption on IHCC were also assessed.

2. Materials and methods

2.1. Chemicals and reagents

All chemicals were purchased from commercial sources and were used without further purification. Distilled water was applied to prepare all solutions and suspensions, which were stored in a dark place

prior to the experiments. The As(V) solutions were prepared from sodium arsenate heptahydrate ($\text{Na}_2\text{HAsO}_4 \cdot 7\text{H}_2\text{O}$) (Neon, Brazil). Fe(III) solutions were produced using ferric nitrate ($\text{Fe}(\text{NO}_3)_3 \cdot 9\text{H}_2\text{O}$) (Synth, Brazil). Hydrochloric acid (37 wt.%) (Fmaia, Brazil), and sodium hydroxide (NaOH) (Neon, Brazil) were used for pH adjustments. All reagents were of analytical grade.

2.2. Raw material and impregnation steps

The corn cob investigated was collected on a farm located in the municipality of Ouro Preto, Minas Gerais, Brazil. Firstly, this material was washed with distilled water and dried in an oven, at 60°C, for 24 hours. A blender (*Mondial, model Vitamaxis filter 500w*) was selected to reduce the particle size and the resulting material was then sieved accordingly. Thus, the particle size fraction between 0.21 mm and 0.15 mm was selected for the subsequent impregnation phase. Based on a literature review (Dupont et al., 2007, Pehlivan et al., 2013b), preliminary tests were performed using different molar concentrations of iron (0.01 mol L⁻¹ to 0.05 mol L⁻¹) and impregnation times (1 to 6 days) to determine the optimal impregnation conditions. The best adsorption capacity for As(V) was achieved when the corncob was impregnated with 0.05 mol L⁻¹ Fe(III), and the experiment lasted 1 day. To ensure uniformity and reduce variability between experiments, a total of 70 g of corn cob were impregnated in the following ratio: for every 1.0 g of corn cob, 100.0 mL of an aqueous solution containing 50 mmol L⁻¹ of ferric nitrate ($\text{Fe}(\text{NO}_3)_3 \cdot 9\text{H}_2\text{O}$) solution were used. Then, sodium hydroxide (6.5 mol L⁻¹) droplets were added slowly to the suspension until pH 11 was attained. This step sought to induce the precipitation of iron(III) hydroxide on the surface of the corn cob particles. The whole experiment was conducted under stirring at 130 rap/min and 25°C, for 24 hours. Subsequently, the suspension was filtered, and the solids were washed with distilled water followed by hydrated ethyl alcohol (92.8%). The resulting material was eventually dried in an oven at 40°C, for 24 hours and stored in a desiccator until further use.

2.3. Characterization of the impregnated corn cob

The characterization of the iron hydroxide-impregnated corn cob was performed in triplicate. This step of the study is detailed in the next sections.

2.3.1. Weight gain ratio

The weight gain observed after the impregnation of corn cob with Fe(III) was determined according to Eq. (1).

$$wg(\%) = \left(\frac{w_{IHCC} - w_C}{w_C} \right) \times 100 \quad (1)$$

where w_g (%) is the relative weight gain, w_{IHCC} (g) and w_C (g) stand for the corn cob weights after and before impregnation with Fe(III), respectively.

2.3.2. Scanning Electron Microscopy (SEM)

Scanning electron microscopy coupled with energy-dispersive X-ray spectroscopy (SEM-EDS) was applied to the following samples: (i) raw corn cob, (ii) IHCC, and (iii) IHCC-As (IHCC after arsenic adsorption) to reveal the chemical composition and morphology of the adsorbent surface. Prior to analysis, these three samples were oven-dried at 333.15 K, for 2 hours and then covered with a thin graphite layer and analysed in a *TESCAN VEGA 3 SEM* microscope. The analyses were carried out under a voltage of 20 keV utilizing a secondary electron detector (SE).

2.3.3. Fourier transform infrared spectroscopy (FTIR)

The samples: (i) raw corn cob, (ii) IHCC, and (iii) IHCC-As were also analysed by FTIR spectroscopy (Nicolet, model Impact 410). A sample weight of 1.0 mg was mixed with 100.0 mg of KBr (spectroscopy grade) and then pressed (Pike Technologies CrushIR, model 181-1110) at 8 Mg for 0.5 min. The 13-mm KBr pellets were analysed in the 400 cm⁻¹ to 4000 cm⁻¹ range, with a resolution of 4 cm⁻¹ and 32 scans per sample.

2.3.4. Point of zero charge (PZC)

In this step, stock sodium chloride (0.1 mol L^{-1}) solutions at pH 2, 3, 4, 5, 6, 7, 8, 9, and 10 were prepared by the addition of either hydrochloric acid (0.1 mol L^{-1}) or sodium hydroxide (0.1 mol L^{-1}). Samples of $50.0 \pm 0.1 \text{ mg}$ IHCC were transferred to 250-mL Erlenmeyer flasks containing 50.0 mL of each solution at different pH values. The flasks were stirred at 150 rap/min and 25°C , for 48 hours. Subsequently, the pH values were measured by a pH meter (*Hanna Instruments, model HI 223*) for the assessment of the pH variation. The pH_{PZC} value was obtained by plotting the intercept of the pH variation curve versus the initial pH. The pH_{PZC} corresponds to the pH value at which the curve obtained touches the zero value on the y-axis (pH variation).

2.4. Effect of pH on arsenic adsorption

The pH influence on arsenic adsorption was determined based on solutions assigning different initial pH values (2, 3, 4, 6, 8, and 10), which were adjusted with either aqueous sodium hydroxide (0.1 mol L^{-1}) or hydrochloric acid (1% (w v⁻¹)) solutions. 100.0 mL of a solution containing 50 mg L^{-1} As(V) along with $100 \pm 0.1 \text{ mg}$ of IHCC were added to 250 mL-Erlenmeyer flasks and then stirred, for 24 hours, in a temperature-controlled shaker (New Brunswick Scientific, model INNOVA 44). The stirring rate was set at 150 rap/min and the selected temperature was $25.0 \pm 1.0^\circ\text{C}$. After the time set, the suspension was filtered through $0.45 \mu\text{m}$ membrane (Millipore). These experiments were performed in duplicate. The aqueous phase had its initial and final As(V) concentrations determined by inductively coupled plasma optical emission spectrometer (ICP-OES) (Agilent, model 725-ES), equipped with a v-groove nebulizer. The equipment operated with an external argon plasma pressure of 6 BAR (5.0 plasma) and an internal pressure of 200 Kpa, with plasma gas flow rate set at 15.0 L min^{-1} along with an auxiliary gas flow rate set at 1.5 L min^{-1} . The wavelength used for arsenic analysis was 188.980 nm. The As(V) loadings on IHCC were calculated by Eq. (2).

$$q_t = \frac{(C_0 - C_t)V}{w} \quad (2)$$

where q_t (mg/g) is the As(V) loading on the solids at time t , C_0 and C_f (mg L^{-1}) are the initial and the final (equilibrium) As(V) concentrations, respectively. V (mL) represents the volume of the solution and w (g) is the weight of IHCC.

2.5. Kinetic studies

The kinetics of arsenic adsorption on IHCC was investigated at $\text{pH } 2.0 \pm 0.1$, which is the pH of maximum adsorption capacity of IHCC, under an initial As(V) concentration of 50 mg L^{-1} . The temperature was set at $25.0 \pm 1.0^\circ\text{C}$ by circulating water in a jacket glass reactor connected to a water bath (*Nova Ética, model 521/2DE*). Stirring was supplied by a digital mechanical mixer (*Ika, model RW 20*).

The effect of the stirring speed on the adsorption kinetics was assessed under the values of 250, 350, 450, and 550 rap/min. Samples of $40 \pm 0.1 \text{ mg}$ of IHCC were mixed with 400.0 mL of As(V) solution in the glass reactor. In these experiments, aliquots of 2.0 mL of the solution were collected at different contact times (5, 10, 20, 30, 60, 90, 120, 150, 180, 210, 240, 270, 300, 330, and 360 minutes). The aliquots were filtered through $0.45 \mu\text{m}$ membrane filters and the As(V) concentrations were determined by ICP-OES. The As(V) loading on IHCC was calculated according to Eq. (2). All experiments were performed in duplicate.

The data were fit to the pseudo-first order (Eq. (3)) and pseudo-second order (Eq. (4)) kinetic models.

$$\ln(q_\infty - q_t) = \ln q_\infty - k_1 t \quad (3)$$

$$\ln(q_\infty - q_t) = \ln q_\infty - k_1 t \quad (4)$$

In Eq. 3 and 4, k_1 (min^{-1}) is the pseudo-first order rate constant; k_2 ($\text{g mg}^{-1} \text{ min}^{-1}$) is the pseudo-second order kinetic rate constant; q_∞ and q_t (mg/g) are, respectively, the solid loadings at infinite time (∞) and at a time t .

The stirring rate value of 450 rap/min was selected for the tests aiming at determining the effect of temperature (25°C , 35°C , 45°C , and 55°C) on the arsenic adsorption kinetics. The data was fit to the pseudo-first and pseudo-second order models. Following, the rate constants were applied in the calculation of the activation energy - in accordance with the Arrhenius equation (Eq. (5)).

$$\ln k_n = \ln A - \frac{E_a}{RT} \quad (5)$$

where k_n represents the rate constant (min^{-1} or $\text{g mol}^{-1} \text{min}^{-1}$); A is the Arrhenius pre-exponential factor (min^{-1}), E_a is the activation energy (J mol^{-1}), R is the ideal gas constant ($8.314 \text{ J mol}^{-1} \text{ K}^{-1}$), and T stands for the absolute temperature (K).

2.6. Equilibrium studies

2.6.1. Adsorption isotherms

Duplicate experiments were carried out in 250 mL-Erlenmeyer flasks containing 100 ± 0.1 mg of IHCC and 100.0 mL of a solution having an initial arsenic concentration ranging from 8 mg L^{-1} to 180 mg L^{-1} , at $\text{pH } 2.0 \pm 0.1$. The flasks were stirred, at 150 rap/min, in a temperature-controlled shaker for 15 hours. The equilibrium data were obtained at temperatures of 25°C , 35°C , and 50°C . At the end of the tests, the As-loaded solids were separated from the solution by filtration. The final concentrations in the aqueous phase were determined by ICP-OES. The amount of arsenic adsorbed in the equilibrium (q_e) was estimated according to Eq. (2). The data obtained were fitted to the Langmuir (Eq. (6)) model, where q_{max} (mg/g) is the maximum arsenic loading on IHCC, b (L mg^{-1}) represents the Langmuir constant, and C_e (mg L^{-1}) stands for the equilibrium arsenic concentration.

$$q_e = \frac{q_{\text{max}} b C_e}{1 + b C_e} \quad (6)$$

2.6.2. Determination of thermodynamic adsorption parameters

The thermodynamic parameters were calculated based on the application of the van't Hoff equation to the thermodynamic equilibrium constant achieved at different temperatures (25°C , 35°C , and 50°C). The thermodynamic equilibrium constants were corrected in accordance with the work by Liu (2006), as depicted in Eq. (7). The detailed approach used to calculate the equilibrium thermodynamic constant can be found in the work of Liu (2009).

$$K_{eq} = \left[\frac{b}{\gamma_e} (1 \text{ mol/L}) \right] \quad (7)$$

In Eq. 7, γ_e is the activity coefficient (dimensionless) at 25°C and b (L mol^{-1}) is the Langmuir constant. The activity coefficient was determined by the extended Debye-Hückel equation (Eq. (8)) for solutions having ionic strengths below 0.1 mol L^{-1} (Lee and Lee, 2019).

$$\log \gamma_e = \frac{-0.509z^2\sqrt{I}}{1 + \frac{\alpha\sqrt{I}}{305}} \quad (8)$$

In Eq. (8), z is the ionic charge, I (mol L^{-1}) is the ionic strength (at equilibrium), and a (pm) is the hydrated ionic radius of As(V) (400 pm).

The corrected thermodynamic equilibrium constant was applied in the determination of the changes in standard enthalpy ($\Delta H^\circ_{\text{ads}}$) and entropy ($\Delta S^\circ_{\text{ads}}$) in accordance with the van't Hoff equation (Eq. (9)).

$$\ln K_{eq} = \frac{\Delta S^\circ_{\text{ads}}}{R} - \frac{\Delta H^\circ_{\text{ads}}}{R} \cdot \frac{1}{T} \quad (9)$$

A plot of $\ln K_{eq}$ versus $1/T$ produces a straight line, in which the angular and linear coefficients are equivalent to $-\Delta H^\circ_{\text{ads}}/R$ and $\Delta S^\circ_{\text{ads}}/R$, respectively.

The change in Gibbs free energy ($\Delta G^\circ_{\text{ads}}$) related to As(V) adsorption on IHCC was calculated by Eq. (10), where R is the gas constant ($8.314 \text{ J mol}^{-1} \text{ K}^{-1}$), and T is the absolute temperature (K).

$$\Delta G^\circ_{\text{ads}} = -RT \ln K_{eq} \quad (10)$$

3. Results and discussion

3.1. Impregnation and characterization of the adsorbent

The impregnation of corn cob particles with iron hydroxides resulted in a weight gain of $27.9 \pm 3.3\%$, due to the precipitation of $\text{Fe}(\text{OH})_3$ on the surface of the IHCC particles. The PZC, the pH value in which the net surface charge is zero, was 6.5 for the IHCC. This means that at pH values below 6.5, the IHCC particles have a positive net surface charge, and at pH values above 6.5 they have a negative net surface charge. A similar result was observed for raw corn cob (PZC = 6.2) by Leyva-Ramos *et al.* (2005).

SEM-EDS micrographs showed the surfaces of (i) raw corn cob, (ii) IHCC, and (iii) IHCC-As, revealing both the iron distribution on the surface of the solid and the arsenate adsorption sites. The impregnation of the surface of corn cob with Fe(III)-hydroxides (Fig. 1) resulted in a substantial change on its surface, from smooth to highly rough, corroborating the findings of Chen *et al.* (2011). The main difference between the elemental composition of (i) raw corn cob and (ii) IHCC was the presence of Fe, which was uniformly distributed on the surface of the material (Fig. 2). In addition, it was also verified that the adsorbed As(V) was evenly distributed on the surface and in the pores of the material (Fig. 3) - as it was also observed for iron. The EDS spectrum showed peaks of Fe impregnated on the surface of the corn cob particle (data not shown), along with arsenic adsorbed on iron-bearing sites.

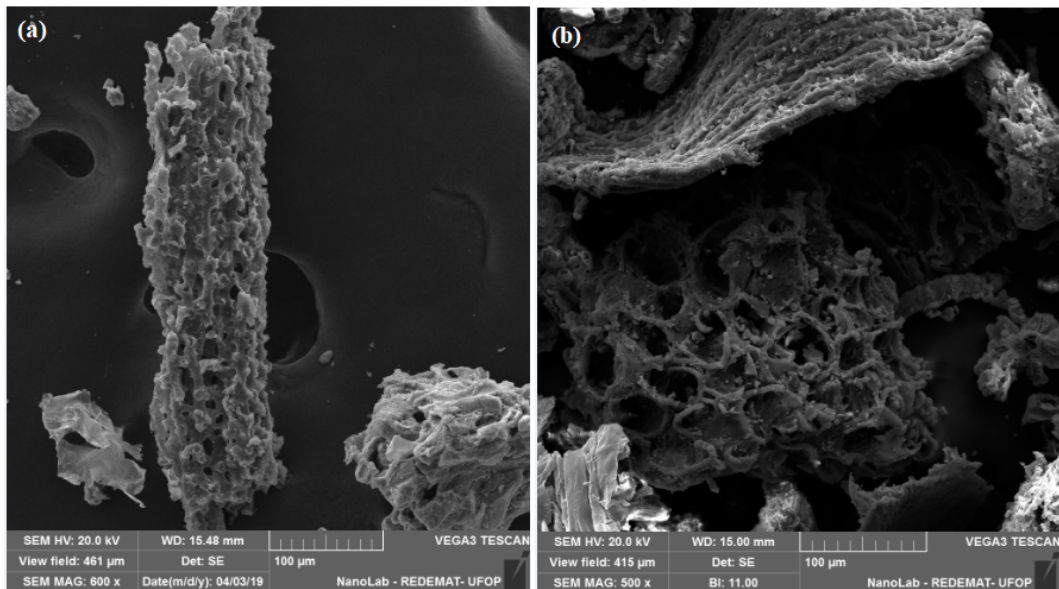


Fig. 1. SEM micrographs of (a) *in natura* corn cob and (b) iron hydroxide impregnated corn cob (IHCC)

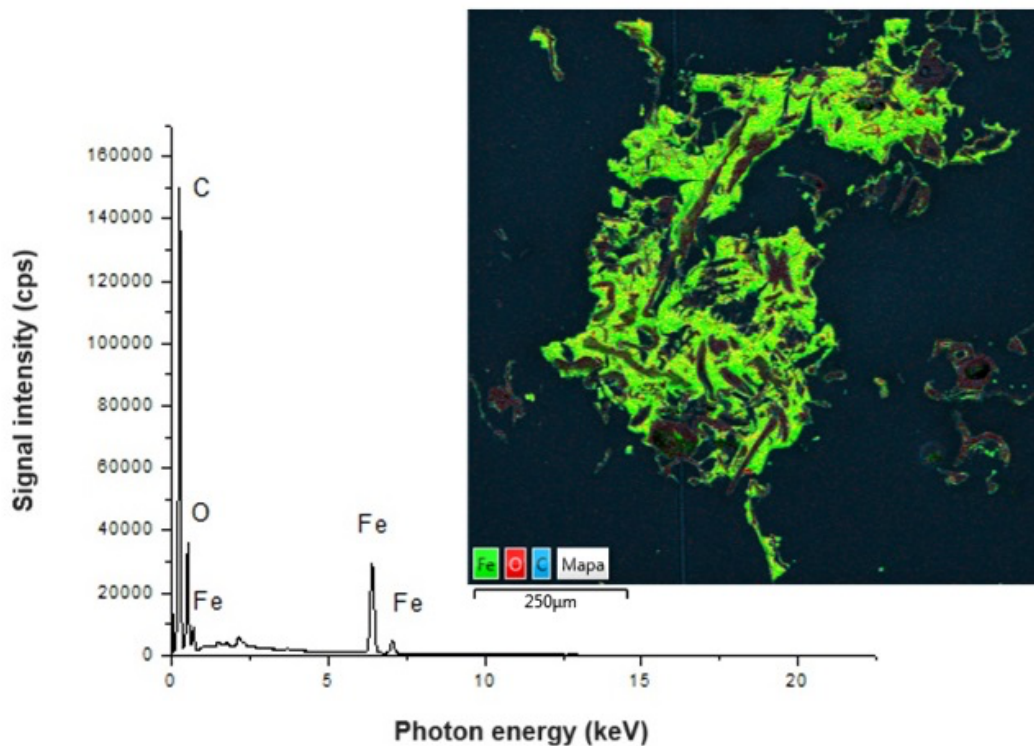


Fig. 2. Energy dispersive X-ray spectroscopy (EDS) elemental map obtained from iron hydroxide impregnated corn cob (IHCC)

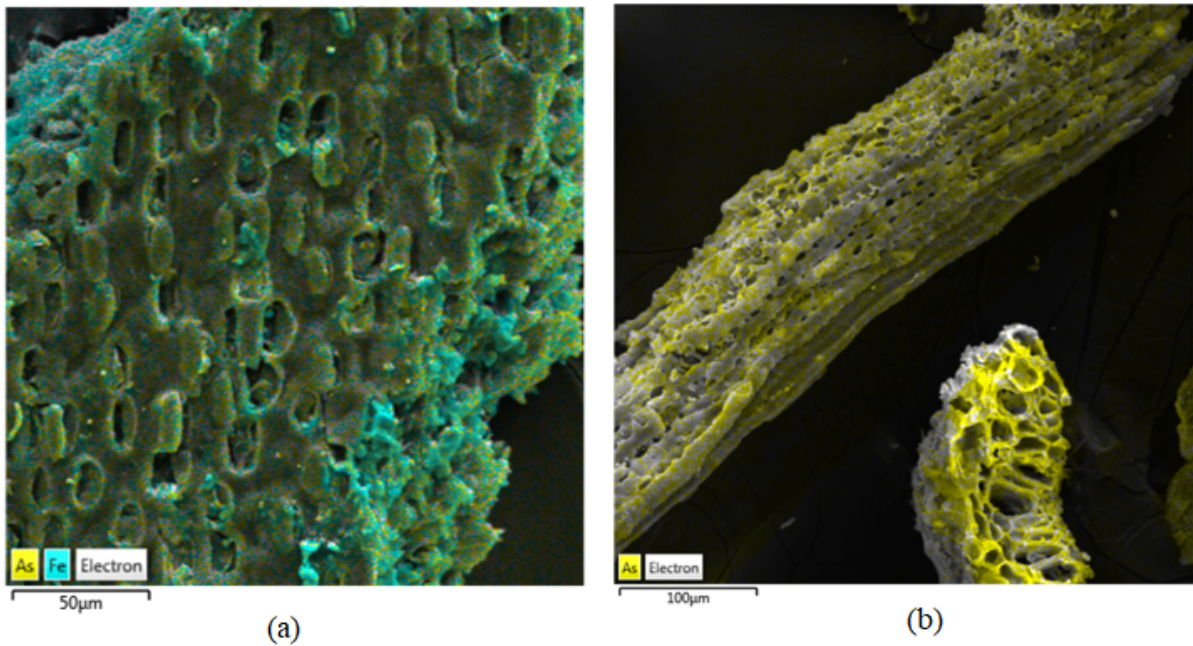


Fig. 3. Energy dispersive X-ray spectroscopy (EDS) elemental maps obtained from (a) As(V) and Fe(III), (b) As(V) on the iron hydroxide impregnated corn cob (IHCC) surface

Fig. 4a shows the FTIR spectra of the raw corn cob, revealing an intense band at 3409 cm^{-1} , attributed to the stretching of the O-H bond present in cellulose, hemicelluloses, and lignin structures (Wang et al., 2012, Lazzari et al., 2018). The vibration at 2916 cm^{-1} is associated to the stretching of the $\text{C}(2\text{sp}^3)\text{-H}$ bond, characteristic of the carbohydrates in cellulose (glucose) and hemicelluloses (xylose and arabinose) (Wang et al., 2012). Moreover, the vibration at 1035 cm^{-1} corresponds to the stretching of C-O bonds in lignin, cellulose, and hemicelluloses (Lazzari et al., 2018). The band at 1631 cm^{-1} corresponds to ketone carbonyl, which is typically present in lignin side chains. In addition, the band at 1728 cm^{-1} indicates the presence of carboxylic acid carbonyl group in hemicelluloses and lignin (Wang et al., 2012, Lazzari et al., 2018).

In the FTIR of IHCC it is observed that the band centred at 3409 cm^{-1} became wider intense than that in the FTIR of raw corn cob (Fig. 4a). Also note that the characteristic peak of the Fe-O bond (580 cm^{-1}) (Gupta and Nayak, 2012) has changed in the IHCC spectrum compared to raw corn cob spectrum. This could be associated with the interaction between hydroxyl group and Fe(III) atom, indicating the modification of the surface of the material by the iron introduction. A similar behaviour was highlighted by Gupta and Nayak (2012), which impregnated orange peel with iron nanoparticles.

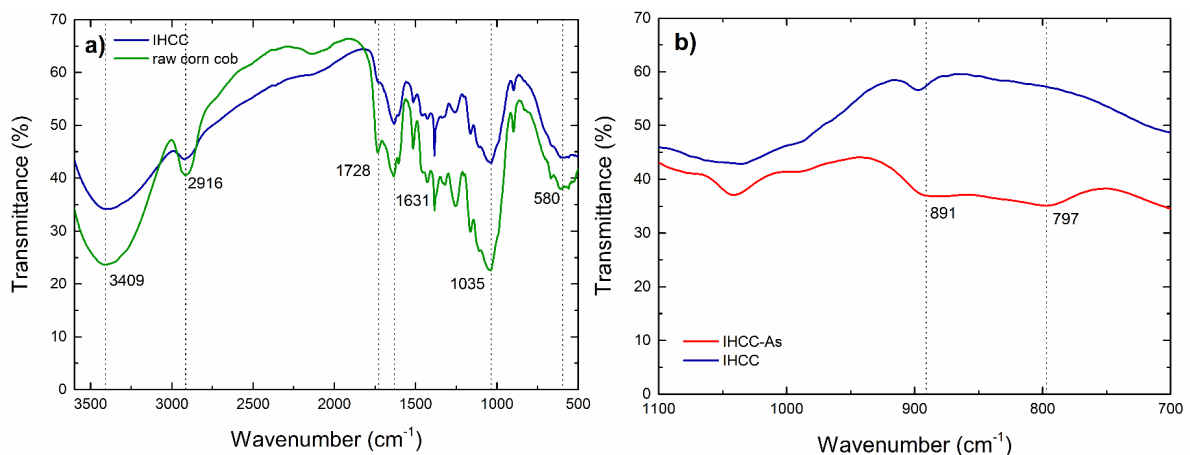


Fig. 4. FTIR spectra of (a) *in natura* corn cob and iron hydroxide impregnated corn cob (IHCC) and (b) IHCC and IHCC after arsenic adsorption (IHCC-As)

After As(V) was adsorbed on the surface of IHCC, two new bands emerged at 797 cm^{-1} and 891 cm^{-1} (Fig. 4b). According to Rijith *et al.* (2012), the former band can be associated with the presence of monodentate iron-arsenic complexes (Fe-O-As). In addition, the band at 891 cm^{-1} is related to the As-O bonding in AsO_4^{3-} ions (Guan *et al.*, 2008). The interaction between Fe(III) and As(V) ions may result in the formation of amorphous scorodite ($\text{FeAsO}_4 \cdot 2\text{H}_2\text{O}$), also known as hydrated Fe(III)-arsenate (Welham *et al.*, 2000), based on the work of Yuan *et al.* (2016), who stated that amorphous ferric arsenate has a weak absorption band at approximately 795 cm^{-1} . Moreover, scorodite (ferric arsenate) presents characteristic absorption bands at 720 cm^{-1} and 795 cm^{-1} (Yuan *et al.*, 2016, Gomez *et al.*, 2010). Therefore, the peak observed at 797 cm^{-1} (Fig. 4b) can be attributed to the monodentate Fe-O-As complex on the surface of IHCC, indicating that scorodite formation possibly occurs (Rijith *et al.*, 2012, Mostafa *et al.*, 2011).

3.2. Effect of pH on arsenic adsorption

The As(V) loading on IHCC observed at different initial pH values (between 2 and 10) are depicted in Table 1, which shows that the solution pH did not vary during the experiments when the initial value was set at 2.0 and 3.0. However, for initial pH values above 4.0, the equilibrium pH tended to be closer to 6.5 (pH_{PZC}).

The As(V) loading on IHCC was reduced as the pH increased, which is consistent with the findings of Tian *et al.* (2011). The highest loadings were observed at pH values between 2 and 4, which corresponded to the pH range in which scorodite is precipitated from aqueous solutions (Welham *et al.*, 2000). A similar result was observed for iron(III)-loaded orange waste, which the highest arsenate removals were achieved at pH values between 2 and 4 (Ghimire *et al.*, 2003). In the pH range 2-3, some hydroxyl groups are protonated, which favours electrostatic adsorption. As the pH increased, the hydroxyl groups on the surface of IHCC were deprotonated, resulting in an increasing repulsion between the negatively charged oxygen atom and aqueous arsenate ions (Toledo *et al.*, 2011). These results suggest that IHCC may be employed as cost-effective solution in the remediation of arsenic-contaminated mine waters.

When the raw corn cob was used for arsenic adsorption, the results showed a much lower capacity (3.27 ± 0.04 mg/g at pH 3.0 and 2.77 ± 0.05 mg/g at pH 2.5, respectively), as compared to the values listed in Table 1, for IHCC. Low adsorption capacities (0.02 mg/g at pH 2.0 and 0.021 mg/g at pH 3.0) were also reported for arsenic adsorption on raw pine leaves by Shafique *et al.* (2012).

Table 1. Effect of pH on the adsorption of arsenate on impregnated corn cob

Initial pH	pH after equilibrium	(mg/g)
2.0	2.02	27.92 ± 0.88
3.0	3.6	23.47 ± 1.16
4.0	6.3	12.13 ± 0.55
6.0	6.8	10.47 ± 1.15
8.0	7.4	5.98 ± 0.92
10.0	8.2	2.46 ± 0.75

3.3. Adsorption kinetics

The effect of the stirring rate on the As(V) adsorption was investigated in the range 250 to 550 rap/min and the film diffusion resistance become negligible when the value of 450 rap/min was reached owing to the reduction in the thickness of the boundary layer (Dotto and Pinto, 2011, Taty-Costodes *et al.*, 2003).

The profile of As(V) adsorption on IHCC fitted well to the pseudo-second order model at 25°C, 35°C, 45°C, and 55°C, as indicated by both high coefficients of determination (R^2) and low values of χ^2_{red} . The activation energy estimated for the adsorption process was 39.35 ± 6.99 kJ mol $^{-1}$, confirming that rate-determining step of the arsenic removal process studied in the current work is chemisorption (Lazaridis and Asouhidou, 2003, Liu, 2006). This value is on a par with the finding (43 kJ mol $^{-1}$) reported by Lakshmpathiraj *et al.* (2006) for the adsorption of arsenate on synthetic goethite. Data fitting to pseudo-

second order model implies that the slowest step of the adsorption process is a chemical reaction, i.e., the binding of As(V) to the adsorption sites (Ho and McKay, 1999). The constant k_2 increased with the increase of temperature, which is consistent with those results of arsenate adsorption on synthetic goethite reported by Lakshmipathiraj *et al.*, (2006). The activation energy estimated for the adsorption process was 39.35 ± 6.99 kJ mol⁻¹, confirming that rate-determining step of the arsenic removal process studied in the current work is chemisorption (Lazaridis and Asouhidou, 2003, Liu, 2006). This value is on a par with the finding (43 kJ mol⁻¹) reported by Lakshmipathiraj *et al.* (2006) for the adsorption of arsenate on synthetic goethite.

3.4. Equilibrium studies

3.4.1. Adsorption isotherms

The Langmuir, Freundlich, Sips, and Dubinin-Radushkevich equations were selected to model the experimental equilibrium data. It is proposed that the Langmuir model, which is classified as an extremely favourable isotherm, provided a better description of the equilibrium data (Fig. 5 and Table 2) (McCabe *et al.*, 2005). Whereas the Sips ($R^2 < 0.85$) and Dubinin-Radushkevich ($R^2 < 0.8$) isotherms did not reveal good fittings, the Freundlich equation described appropriately the adsorption data only at 25°C ($R^2 = 0.93$). On the other hand, the Langmuir equation represented well the arsenic adsorption at all temperature tested ($R^2 > 0.9$).

The value of the Langmuir constant (b) increased with the temperature (Table 2), which means that the affinity of the adsorption sites for As(V) also increased with the temperature (between 25°C and 50°C).

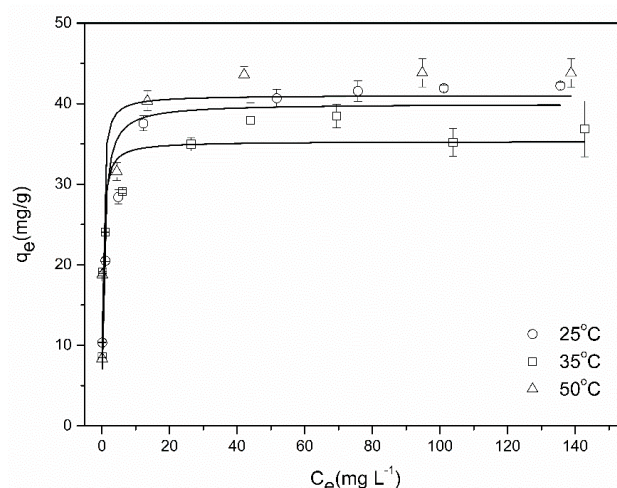


Fig. 5. Adsorption Langmuir isotherms of As(V) onto for 15 hours of contact at pH 2.0 and stirring of 150 rap/min at 25°C, 35°C, and 50°C

Table 2. Kinetic parameters obtained for the arsenic adsorption in the IHCC, at different temperatures, pH 2.0, with initial arsenic concentration of 50 mg L⁻¹, agitation 450 rap/min

Kinetic model	Parameters	Temperature (°C)			
		25	35	45	55
Pseudo first order	q_e (mg/g)	18.61±0.70	19.66±0.91	14.14±0.68	18.04±0.02
	k_1 (min ⁻¹)	0.081±0.009	0.093±0.014	0.125±0.026	0.179±0.002
	R^2	0.96	0.96	0.91	0.94
	χ^2_{red}	1.454	2.079	2.283	0.366
Pseudo second order	q_e (mg/g)	20.12±1.84	21.62±0.85	15.28±0.66	19.08±0.32
	k_2 (g mg ⁻¹ min ⁻¹)	4.5x10 ⁻³	6.1x10 ⁻³	1.33x10 ⁻³	1.66x10 ⁻³
		3±1.8x10 ⁻³	3±1.1x10 ⁻³	2±3.78x10 ⁻³	2±2.11x10 ⁻³
	R^2	0.92	0.98	0.95	0.99
	χ^2_{red}	4.228	0.983	1.249	0.267

At equilibrium, the maximum adsorption capacity of As(V) on IHCC, at the temperature range investigated, was higher than the values reported in literature for Fe₃O₄-impregnated wheat straw at pH 3.0 (3.25 mg/g) (Tian et al., 2011) and ferric nitrate-modified sugarcane bagasse at pH 4.0 (22.1 mg/g) (Pehlivan et al., 2013b).

The adsorption capacity of the iron hydroxide impregnated corn cob (Table 3) was very similar to other iron-impregnated materials. At acidic pH, the performance of this material was equivalent to the performance achieved by the iron-impregnated activated carbon (Rahman et al., 2019). Despite the significant reduction in the adsorption capacity of IHCC at neutral pH, the removal efficiency achieved is reasonable, having been slightly higher than the performance of chitosan (Kloster et al., 2020) and vermiculite (Mondal and Ray, 2020) modified with iron oxides. In addition, this biosorbent is promising due to its low cost, easy acquisition, and can be easily separated from the reaction medium after treatment.

Table 3. Parameters of the adsorption isotherms at different temperatures, pH=2.0 for the adsorption of As(V) in the IHCC

Isotherm model	Parameters	Temperature (°C)		
		25	35	50
Langmuir	q_{\max} (mg/g)	40.00±2.51	35.32±1.40	41.05±2.88
	b (L mg ⁻¹)	1.80±0.67	3.13±0.66	3.99±0.9
	b (L mol ⁻¹)	141601.82±50197.47	234504.61±49448.26	298937.18±67429.44
	R^2	0.90	0.95	0.91
	χ^2_{red}	0.818	0.330	0.946

3.4.2. Adsorption thermodynamic parameters

The equilibrium data were used to plot the $\ln(K_{\text{eq}})$ versus $1/T$ graph. As the temperature increased the $\Delta G^{\circ}_{\text{ads}}$ value became more negative, as can be seen in Table 4, confirming the spontaneity of adsorption (Shahwan, 2021), as expected. The value of the term $T\Delta S^{\circ}_{\text{ads}}$ was positive (53.67 kJ mol⁻¹) and higher than that of $\Delta H^{\circ}_{\text{ads}}$ (23.82 kJ mol⁻¹), indicating that the adsorption process of As(V) on IHCC was entropically driven. The positive value of $\Delta S^{\circ}_{\text{ads}}$ indicated that the number of degrees of freedom of the system increased after As(V) adsorption on IHCC (Pereira et al., 2020). This suggests that water molecules were released from the hydration shell of the As(V) ions and the adsorption sites to the bulk solution, as the Fe-O-As complex was formed on the surface of IHCC (Anastopoulos and Kyzas, 2016). This statement is supported by the observation that the AsO₄³⁻ ion is coordinated by 10-11 water molecules (Pathak and Bandyopadhyay, 2016). The $\Delta H^{\circ}_{\text{ads}}$ value was positive, which characterized an endothermic adsorption process. According to Herrag *et al.* (2008), the $\Delta H^{\circ}_{\text{ads}}$ values of under 20 kJ mol⁻¹ indicates physical adsorption. The $\Delta H^{\circ}_{\text{ads}}$ value determined in the current study was 23.82±5.21 kJ mol⁻¹. This value could be associated with mixed interactions involved in the As(V) adsorption on IHCC, i.e., electrostatic adsorption (physisorption) and chemisorption.

Therefore, there is evidence that the mechanisms involved in As(V) removal by IHCC were complexation and electrostatic interactions between the positively charged IHCC surface ($\equiv\text{FeOH}^{2+}$) and the anionic As(V) species (Maia et al., 2021).

Table 4. Thermodynamic parameters of the As(V) adsorption process in IHCC

Temperature (°C)	$\ln K_{\text{eq}}$	$\Delta H^{\circ}_{\text{ads}}$ (kJ mol ⁻¹)	$\Delta S^{\circ}_{\text{ads}}$ (kJ mol ⁻¹ .K ⁻¹)	$\Delta G^{\circ}_{\text{ads}}$ (kJ mol ⁻¹)
25	14.64			-36.28
35	15.12	+23.82±5.21	+0.18±0.01	-38.74
50	15.39			-41.37

4. Conclusions

Corn cob, which had an original As(V) adsorption capacity of 2.77 mg/g in its raw form was modified with ferric iron to improve its adsorption capacity. As a result, the impregnated corn cob (IHCC) had

its adsorption capacity increased to 40.0 mg/g (at 25°C). In addition, the IHCC was efficient in the removal of arsenic from acidic solutions, mainly those having pH values between 2 and 3 suggesting that IHCC may be applied in the treatment of industrial and mining effluents containing arsenic. Kinetic studies revealed that equilibrium was reached within 2 hours and arsenic adsorption was a best described by the pseudo-second order model with an activation energy assigning 39.35 ± 6.99 kJ mol⁻¹. These data suggests that chemical reaction was the controlling step of the kinetics of arsenic adsorption by IHCC. Equilibrium experiments showed that arsenic adsorption on IHCC was (i) an entropically driven and (ii) endothermic phenomenon. The standard change in enthalpy of adsorption (23.82 kJ mol⁻¹) was characteristic of a mixed interaction process comprising electrostatic adsorption and chemisorption. In addition, the presence of a monodentated complex between As(V) and Fe(III) was suggested by infrared spectroscopy. Therefore, the use of this low-cost adsorbent (IHCC) for arsenic removal is a promising technology to be used as a complementary treatment of arsenic-bearing effluents.

Acknowledgments

The authors are grateful to Federal University of Ouro Preto and the following agencies for their financial support: Coordination of Improvement of Higher Education Personnel (CAPES), National Council for Scientific and Technological Development (CNPq), Funding Authority for Studies and Projects (Finep) and The Research Support Foundation of the State of Minas Gerais (FAPEMIG).

References

- ALKA, S., SHAHIR, S., IBRAHIM, N., NDEJIKO, M. J., VO, D.-V. N., MANAN, F. A., 2021. *Arsenic removal technologies and future trends: A mini review*. J. Clean. Prod. 278, 123805.
- ANASTOPOULOS, I., KYZAS, G. Z., 2016. *Are the thermodynamic parameters correctly estimated in liquid-phase adsorption phenomena?* J. Mol. Liq. 218, 174-185.
- BRAINER, M. S. C. P., 2021. *Coco: produção e mercado*. Caderno Setorial ETENE; Banco do Nordeste do Brasil: Fortaleza, Brazil, 206, 1-13.
- BYAMBAA, E., SEON, J., KIM, T.-H., KIM, S. D., JI, W. H., HWANG, Y., 2021. *Arsenic (V) Removal by an Adsorbent Material Derived from Acid Mine Drainage Sludge*. Appl. Sci. 11, 47.
- CHEN, R., ZHI, C., YANG, H., BANDO, Y., ZHANG, Z., SUGIUR, N., GOLBERG, D., 2011. *Arsenic (V) adsorption on Fe₃O₄ nanoparticle-coated boron nitride nanotubes*. J. Colloid Interface Sci. 359, 261-268.
- CONAB 2021. *Acompanhamento da safra brasileira de grãos*. Ministério da agricultura, pecuária e abastecimento, Brasília, Brazil.
- COPE, C. O., WEBSTER, D. S., SABATINI, D. A., 2014. *Arsenate adsorption onto iron oxide amended rice husk char*. Sci. Total Environ. 488, 554-561.
- DESCHAMPS, E., CIMINELLI, V. S. T., WEIDLER, P. G., RAMOS, A. Y., 2003. *Arsenic sorption onto soils enriched in Mn and Fe minerals*. Clays Clay Miner. 51, 197-204.
- DESCHAMPS, E., MATSCHULLAT, J., 2007. *Arsênio antropogênico e natural: um estudo em regiões do Quadrilátero Ferrífero*. Fundação Estadual do Meio Ambiente, Belo Horizonte, Brazil.
- DOTTO, G. L., PINTO, L. A. A., 2011. *Adsorption of food dyes acid blue 9 and food yellow 3 onto chitosan: Stirring rate effect in kinetics and mechanism*. J. Hazard. Mater. 187, 164-170.
- DUPONT, L., JOLLY, G., APLINCOURT, M., 2007. *Arsenic adsorption on lignocellulosic substrate loaded with ferric ion*. Environ. Chem. Lett. 5, 125-129.
- GHIMIRE, K. N., INOUE, K., YAMAGUCHI, H., MAKINO, K., MIYAJIMA, T. 2003. *Adsorptive separation of arsenate and arsenite anions from aqueous medium by using orange waste*. Water Res. 37, 4945-4953.
- GOMEZ, M. A., ASSAAOUDI, H., BECZE, L., CUTLER, J. N., DEMOPOULOS, G. P., 2010. *Vibrational spectroscopy study of hydrothermally produced scorodite (FeAsO₄·2H₂O), ferric arsenate sub-hydrate (FAsH; FeAsO₄·0.75H₂O) and basic ferric arsenate sulfate (BFAS; Fe[(AsO₄)_{1-x}(SO₄)_x(OH)_x]·wH₂O)*. J. Raman Spectrosc. 41, 212-221.
- GUAN, X.-H., WANG, J., CHUSUEI, C. C., 2008. *Removal of arsenic from water using granular ferric hydroxide: Macroscopic and microscopic studies*. J. Hazard. Mater. 156, 178-185.
- GUPTA, V. K., NAYAK, A., 2012. *Cadmium removal and recovery from aqueous solutions by novel adsorbents prepared from orange peel and Fe₂O₃ nanoparticles*. Chem. Eng. J. 180, 81-90.

- HERRAG, L., CHETOUANI, A., ELKADIRI, S., HAMMOUTI, B., AOUNITI, A., 2008. *Pyrazole derivatives as corrosion inhibitors for steel in hydrochloric acid*. *Port. Electrochim. Acta.* 26, 211-220.
- HO, Y. S., MCKAY, G. 1999. *Pseudo-second order model for sorption processes*. *Process Biochem.* 34, 451-465.
- KLOSTER, G. A., VALIENTE, M., MARCOVICH, N. E., MOSIEWICKI, M. A., 2020. *Adsorption of arsenic onto films based on chitosan and chitosan/nano-iron oxide*. *Int. J. Biol. Macromol.* 165, 1286-1295.
- LADEIRA, A. C. Q., CIMINELLI, V. N. S. T., 2004. *Adsorption and desorption of arsenic on an oxisol and its constituents*. *Water Res.* 38, 2087-2094.
- LAKSHMIPATHIRAJ, P., NARASIMHAN, B. R. V., PRABHAKAR, S., BHASKAR RAJU, G., 2006. *Adsorption of arsenate on synthetic goethite from aqueous solutions*. *J. Hazard. Mater.* 136, 281-287.
- LAZARIDIS, N. K., ASOUHIDOU, D. D., 2003. *Kinetics of sorptive removal of chromium(VI) from aqueous solutions by calcined Mg-Al-CO₃ hydrotalcite*. *Water Res.* 37, 2875-2882.
- LAZZARI, E., SCHENA, T., MARCELO, M. C. A., PRIMAZ, C. T., SILVA, A. N., FERRÃO, M. F., BJERK, T., CARAMÃO, E. B., 2018. *Classification of biomass through their pyrolytic bio-oil composition using FTIR and PCA analysis*. *Ind. Crop. Prod.* 111, 856-864.
- LEE, K. S., LEE, J. H., 2019. *Hybrid enhanced oil recovery using smart waterflooding*, Gulf Professional Publishing Houston, USA.
- LEYVA-RAMOS, R., BERNAL-JACOME, L. A., ACOSTA-RODRIGUEZ, I., 2005. *Adsorption of cadmium(II) from aqueous solution on natural and oxidized corncob*. *Sep. Purif. Technol.* 45, 41-49.
- LIU, Y., 2006. *Some consideration on the Langmuir isotherm equation*. *Colloids Surfaces A Physicochem. Eng. Asp.* 274, 34-36.
- LIU, Y., 2009. *Is the Free Energy Change of Adsorption Correctly Calculated?* *J. Chem. Eng. Data.* 54, 1981-1985.
- MAIA, L. C., SOARES, L. C., ALVES GURGEL, L. V., 2021. *A review on the use of lignocellulosic materials for arsenic adsorption*. *J. Environ. Manage.* 288, 112397.
- MCCABE, W. L., SMITH, J. C., HARRIOTT, P., 2005. *Unit operations of chemical engineering*, McGraw-Hill's Science, New York, USA.
- MOHAN, D., CHANDER, S., 2006. *Removal and recovery of metal ions from acid mine drainage using lignite - A low cost sorbent*. *J. Hazard. Mater.* 137, 1545-1553.
- MOHAN, D., PITTMAN, C. U., 2007. *Arsenic removal from water/wastewater using adsorbents - A critical review*. *J. Hazard. Mater.* 142, 1-53.
- MONDAL, M., RAY, A. K., 2020. *Removal of As(V) using low cost adsorbents: aerocrete and vermiculite modified with iron oxy-hydroxide*. *Adsorption.* 26, 387-396.
- MOSTAFA, M. G., CHEN, Y.-H., JEAN, J.-S., LIU, C.-C., LEE, Y.-C., 2011. *Kinetics and mechanism of arsenate removal by nanosized iron oxide-coated perlite*. *J. Hazard. Mater.* 187, 89-95.
- NASHINE, A., TEMBHURKAR, A., 2016. *Iron oxide impregnated sugarcane bagasse waste material as sorbent for As(III) removal from water: kinetic, equilibrium and thermodynamic studies*. *J. Water Supply Res. Technol.* 65, 645-652.
- ODLING, G., CHATZISYMEON, E., KARVE, P., OGALE, S., IVATURI, A., ROBERTSON, N., 2020. *Naturally derived carbon for E. coli and arsenic removal from water in rural India*. *Environ. Technol. Innov.* 18, 100661.
- PATHAK, A. K., BANDYOPADHYAY, T., 2016. *Solvation of arsenate anion: combined quantum mechanics and molecular dynamics based investigation*. *Mol. Phys.* 114, 2029-2036.
- PEHLIVAN, E., TRAN, H. T., OUÉDRAOGO, W. K. I., SCHMIDT, C., ZACHMANN, D., BAHADIR, M., 2013a. *Sugarcane bagasse treated with hydrous ferric oxide as a potential adsorbent for the removal of As(V) from aqueous solutions*. *Food Chem.* 138, 133-138.
- PEHLIVAN, E., TRAN, T. H., OUÉDRAOGO, W. K. I., SCHMIDT, C., ZACHMANN, D., BAHADIR, M., 2013b. *Removal of As(V) from aqueous solutions by iron coated rice husk*. *Fuel Process. Technol.* 106, 511-517.
- PEREIRA, A. R., SOARES, L. C., TEODORO, F. S., ELIAS, M. M. C., FERREIRA, G. M. D., SAVEDRA, R. M. L., SIQUEIRA, M. F., MARTINEAU-CORCOS, C., DA SILVA, L. H. M., PRIM, D., GURGEL, L. V. A., 2020. *Aminated cellulose as a versatile adsorbent for batch removal of As(V) and Cu(II) from mono- and multicomponent aqueous solutions*. *J. Colloid Interface Sci.* 576, 158-175.
- RAHMAN, H. L., ERDEM, H., SAHIN, M., ERDEM, M., 2019. *Iron-Incorporated Activated Carbon Synthesis from Biomass Mixture for Enhanced Arsenic Adsorption*. *Water. Air. Soil Pollut.* 231, 6.
- RIJITH, S., ANIRUDHAN, T. S., SHRIPATHI, T., 2012. *Evaluation of Iron(III) Chelated Polymer Grafted Lignocellulosics for Arsenic(V) Adsorption in a Batch Reactor System*. *Ind. Eng. Chem. Res.* 51, 10682-10694.

- SANYANG, M., GHANI, W. A. W. A. K., IDRIS, A., AHMAD, M. B., 2016. *Hydrogel biochar composite for arsenic removal from wastewater*. *Desalin. Water Treat.* 57, 3674–3688.
- SCHNEIDER, V. E., PERESIN, D., TRENTIN, A. C., BORTOLIN, T. A., SAMBUICHI, R. H. R., 2012. *Diagnóstico dos resíduos orgânicos do setor agrossilvopastoril e agroindustriais associadas*. Available from: <https://repositorio.ipea.gov.br/handle/11058/7687>. Accessed May 15, 2024.
- SEN GUPTA, S., BHATTACHARYYA, K. G., 2011. *Kinetics of adsorption of metal ions on inorganic materials: A review*. *Adv. Colloid Interface Sci.* 162, 39-58.
- SHAFIQUE, U., IJAZ, A., SALMAN, M., ZAMAN, W. U., JAMIL, N., REHMAN, R., JAVAID, A., 2012. *Removal of arsenic from water using pine leaves*. *J. Taiwan Inst. Chem. Eng.* 43, 256-263.
- SHAHWAN, T., 2021. *Critical insights into the limitations and interpretations of the determination of ΔG_0 , ΔH_0 , and ΔS_0 of sorption of aqueous pollutants on different sorbents*. *Colloids Interface Sci. Commun.* 41, 100369.
- SMITH, A. H., LINGAS, E. O., RAHMAN, M., 2000. *Contamination of drinking-water by arsenic in Bangladesh: a public health emergency*. *Bull. World Health Organ.* 78, 1093-1103.
- SUD, D., MAHAJAN, G., KAUR, M. P., 2008. *Agricultural waste material as potential adsorbent for sequestering heavy metal ions from aqueous solutions – A review*. *Bioresour. Technol.* 99, 6017-6027.
- TATY-COSTODES, V. C., FAUDUET, H., PORTE, C., DELACROIX, A., 2003. *Removal of Cd(II) and Pb(II) ions, from aqueous solutions, by adsorption onto sawdust of Pinus sylvestris*. *J. Hazard. Mater.* 105, 121-142.
- TIAN, Y., WU, M., LIN, X., HUANG, P., HUANG, Y., 2011. *Synthesis of magnetic wheat straw for arsenic adsorption*. *J. Hazard. Mater.* 193, 10-16.
- TOLEDO, T. V., BELLATO, C. R., ROSÁRIO, R. H. D., MARQUES NETO, J. D. O., 2011. *Adsorção de arsênio (V) pelo composto magnético hidrotalcita: óxido de ferro*. *Quím. Nova.* 34, 561-567.
- VIDAL, M. F., 2021. *Produção de laranja na área de atuação do BNB*. *Caderno Setorial ETENE; Banco do Nordeste do Brasil: Fortaleza, Brazil*, 198, 1-14.
- WANG, J., ZHENG, Y., WANG, A., 2012. *Effect of kapok fiber treated with various solvents on oil absorbency*. *Ind. Crop. Prod.* 40, 178-184.
- WANG, S., GAO, B., LI, Y., CREAMER, A. E., HE, F., 2017. *Adsorptive removal of arsenate from aqueous solutions by biochar supported zero-valent iron nanocomposite: Batch and continuous flow tests*. *J. Hazardous Mater.* 322 (Part A), 172–181.
- WANG, S., GAO, B., ZIMMERMAN, A. R., LI, Y., MA, L., HARRIS, W. G., MIGLIACCIO, K. W., 2015. *Removal of arsenic by magnetic biochar prepared from pinewood and natural hematite*. *Bioresour. Technol.* 175, 391–395.
- WARWICK, M., MARCELO, C., MARCELO, C., SHAW, J., QAYYUM, R., 2021. *The relationship between chronic arsenic exposure and body measures among US adults: National Health and Nutrition Examination Survey 2009-2016*. *J. Trace Elem. Med. Biol.* 67, 126771.
- WELHAM, N. J., MALATT, K. A., VUKCEVIC, S., 2000. *The stability of iron phases presently used for disposal from metallurgical systems – A review*. *Miner. Eng.* 13, 911-931.
- WHO, World Health Organization, 2001. *Environmental Health Criteria 224: Arsenic and arsenic compounds* Geneve. Available from: <https://www.inchem.org/documents/ehc/ehc/ehc224.htm>. Accessed January 15, 2024.
- WHO, World Health Organization, 2023. *Arsenic* [Online]. Geneve. Available from: <https://www.who.int/news-room/fact-sheets/detail/arsenic>. Accessed May 13, 2023.
- YUAN, Z., ZHANG, D., WANG, S., XU, L., WANG, K., SONG, Y., XIAO, F., JIA, Y., 2016. *Effect of hydroquinone-induced iron reduction on the stability of scorodite and arsenic mobilization*. *Hydrometallurgy.* 164, 228-237.
- ZHANG, M., GAO, B., 2013. *Removal of arsenic, methylene blue, and phosphate by biochar/AlOOH nanocomposite*. *Chem. Eng. J.* 226, 286–292.
- ZIGLIO, B. R., BEZERRA, J. R. M. V., BRANCO, I. G., BASTOS, R., RIGO, M., 2007. *Elaboração de pães com adição de farinha de sabugo de milho*. *Rev. Ciências Exatas e Nat.* 9.